MNRAS 000, 1–12 (2018) Preprint 3 May 2018 Compiled using MNRAS LATEX style file v3.0

A new physical interpretation of optical and infrared variability in quasars

Nicholas P. Ross[1]★, K. E. Saavik Ford[2,3,4], Matthew Graham[5], Barry McKernan[2,3,4], Daniel Stern[6], Aaron M. Meisner[7,8], Roberto J. Assef[9], Arjun Dey[10], Andrew J. Drake[11], Hyunsung D. Jun[12], Dustin Lang[13,14,15]

[1]*Institute for Astronomy, University of Edinburgh, Royal Observatory, Blackford Hill, Edinburgh EH9 3HJ, United Kingdom*
[2]*Department of Science, BMCC, City University of New York, New York, NY 10007, USA*
[3]*Department of Astrophysics, Rose Center for Earth and Space, American Museum of Natural History, Central Park West at 79th Street, NY 10024, USA*
[4]*Graduate Center, City University of New York, 365 5th Avenue, New York, NY 10016, USA*
[5]*Cahill Center for Astronomy and Astrophysics, California Institute of Technology, Mail Code 249/17, 1200 E California Blvd, Pasadena CA 91125, USA*
[6]*Jet Propulsion Laboratory, California Institute of Technology, 4800 Oak Grove Drive, Mail Stop 169-221, Pasadena, CA 91109, USA*
[7]*Lawrence Berkeley National Laboratory, 1 Cyclotron Road, Berkeley, CA 92420, U.S.A.*
[8]*Berkeley Center for Cosmological Physics, Berkeley, CA 94720, USA*
[9]*Núcleo de Astronomía de la Facultad de Ingeniería y Ciencias, Universidad Diego Portales, Av. Ejército Libertador 441, Santiago, Chile.*
[10]*National Optical Astronomy Observatory, 950 N. Cherry Ave, Tucson, AZ 85719, USA*
[11]*Center for Advanced Computing Research, California Institute of Technology, 1200 E California Blvd, Pasadena CA 91125, USA*
[12]*School of Physics, Korea Institute for Advanced Study, 85 Hoegiro, Dongdaemun-gu, Seoul 02455, Korea*
[13]*Dunlap Institute, University of Toronto, Toronto, ON M5S 3H4, Canada*
[14]*Department of Astronomy & Astrophysics, University of Toronto, Toronto, ON M5S 3H4, Canada*
[15]*Perimeter Institute for Theoretical Physics, Waterloo, ON N2L 2Y5, Canada*

Accepted XXX. Received YYY; in original form ZZZ

ABSTRACT

Changing-look quasars are a recently identified class of active galaxies in which the strong UV continuum and/or broad optical hydrogen emission lines associated with unobscured quasars either appear or disappear on timescales of months to years. The physical processes responsible for this behaviour are still debated, but changes in the black hole accretion rate or accretion disk structure appear more likely than changes in obscuration. Here we report on four epochs of spectroscopy of SDSS J110057.70-005304.5, a quasar at a redshift of $z = 0.378$ whose UV continuum and broad hydrogen emission lines have faded, and then returned over the past ≈20 years. The change in this quasar was initially identified in the infrared, and an archival spectrum from 2010 shows an intermediate phase of the transition during which the flux below rest-frame ≈3400Å has decreased by close to an order of magnitude. This combination is unique compared to previously published examples of changing-look quasars, and is best explained by dramatic changes in the innermost regions of the accretion disk. The optical continuum has been rising since mid-2016, leading to a prediction of a rise in hydrogen emission line flux in the next year. **Increases in the infrared flux are beginning to follow**, occurring on a ∼3 year observed timescale. If our model is confirmed, the physics of changing-look quasars are governed by processes at the innermost stable circular orbit (ISCO) around the black hole, and the structure of the innermost disk. The easily identifiable and monitored changing-look quasars would then provide a new probe and laboratory of the nuclear central engine.

Key words: accretion, accretion discs – surveys – quasars: general

1 INTRODUCTION

The Shakura-Sunyaev α−disk model (Shakura & Sunyaev 1973) has long been used to describe the basic properties of the optically thick, geometrically thin accretion disks expected to orbit the supermassive black holes at the nuclei of quasars. This accretion disk is thought to be the origin of thermal continuum emission observed in the rest-frame ultraviolet and optical. The thermal emission seen in the infrared spectrum of quasars is believed to originate from molecular dust outside the accretion

★ E-mail: npross@roe.ac.uk

disk and traditional broadline region (BLR). Thus, the IR flux is directly proportional to the emission from the disk, reprocessed by the dusty reservoir and delayed by the light-travel time between the two (see e.g., Antonucci 1993; Perlman et al. 2008; Lasota 2016, for reviews). As such, the thermal accretion disk photons are the seeds for both the X-ray emission – due to Compton-upscattering in the corona (e.g., Begelman et al. 1983; Risaliti et al. 2009; Lusso & Risaliti 2017) and the thermal mid-IR emission from the torus.

The α-disk model assumes that the disk is geometrically thin (i.e., $h/r \ll 1$ where h/r is the disk aspect ratio) and that angular momentum is transported by a kinematic viscosity, ν, parametrized by Shakura & Sunyaev (1973) as $\nu = \alpha c_s h$ where c_s is the local mean sound speed in the disk and h is the scale-height perpendicular to the disk plane. The thermal emission need not be, but often is, treated as a superposition of blackbodies at varying annuli with an effective temperature dependence[1] going as $T(r) \propto r^{-3/4}$.

Given the size scales and temperatures associated with supermassive black holes, a substantial fraction of the bolometric luminosity should be in the form of UV photons – the so-called "Big Blue Bump" (Shields 1978; Malkan & Sargent 1982). For the optically thick, UV emitting disk to accrete onto the black hole, substantial angular momentum must be lost. The kinematic viscosity of the plasma, α, seems the likely mechanism that transports angular momentum outward. This viscosity is likely due to magnetorotational instability (MRI; Balbus & Hawley 1991) with additional contributions to turbulence from the effects of objects embedded in the disk (e.g., McKernan et al. 2014).

However, as has long been established (e.g., Alloin et al. 1985) and recently re-visited (e.g., LaMassa et al. 2015; Runnoe et al. 2016; MacLeod et al. 2016; Ruan et al. 2016; Rumbaugh et al. 2017; Yang et al. 2017; Lawrence 2018), the observation of even slowly varying Balmer emission lines in quasars strongly suggests that if a thermal accretion disk does indeed contribute substantially to the ionizing or optical continuum, then it cannot be in quasi-steady state equilibrium. The variations must be due to more chaotic disturbances or instabilities in the disk that propagate at considerably higher speeds than the radial accretion flow and possibly as fast as the orbital velocity.

Furthermore as e.g., Koratkar & Blaes (1999) and Sirko & Goodman (2003) among others point out, the observed spectral energy distributions (SEDs) of typical quasars differ markedly from classical α-disk theoretical predictions (Shakura & Sunyaev 1973; Pringle 1981) with a typical observed quasar SED flat in λF_λ over several decades in wavelength (Elvis et al. 1994; Richards et al. 2006). Also, real AGN disks seem to be cooler (e.g., Lawrence 2012) and larger (e.g., Pooley et al. 2007; Morgan et al. 2010, 2012; Mosquera & Kochanek 2011) than the α-disk model predicts. The α-disk is an ad hoc parameterization of disk viscosity and does not permit predictions of global changes from local perturbations (King 2012).

Nevertheless, in this paper, we utilize the mathematically simple α-disk model as a framework and departure point for our own disk models. Here, we build on previous work (Sirko & Goodman 2003; Zimmerman et al. 2005; Hameury et al. 2009) and introduce a phenomenological model which does allow changes across the accretion disk and, crucially, makes predictions which can be observed in the SED.

Changing-look quasars (CLQs) are luminous active galaxies in which the strong UV continuum and/or broad optical hydrogen emission lines associated with unobscured quasars either appear or disappear on timescales of months to years. CLQs have traditionally been discovered by looking for large, $|\Delta m| > 1$ magnitude changes in the optical light curves of quasars or galaxies. In contrast, we have taken advantage of the ongoing mid-IR Near-Earth Object Wide-Field Infrared Survey Explorer Reactivation mission (NEOWISE-R; Mainzer et al. 2014; Meisner et al. 2017b,a), supplemented with the optical Dark Energy Camera Legacy Survey (DECaLS[2]), in order to discover new changing-look quasars. While previous efforts have used the 1-year baseline of the WISE mission to identify changing-look quasars (e.g., Assef et al. 2018; Stern et al. 2018), our investigation is the first to extend this selection to the infrared using NEOWISE-R mission data. We have identified a sample of Sloan Digital Sky Survey (SDSS) quasars that show significant changes in their IR flux over the course of a few years. Importantly, our IR light curves enable us to set limits on SED changes due to obscuration.

In this article we present the $z = 0.378$ quasar SDSS J110057.70-005304.5 (hereafter J1100-0053). J1100-0053 was a known quasar we identified as interesting due to its IR light curve. We have spectral observations for J1100-0053 showing a transition in the blue-continuum into a 'dim state' where the rest-frame UV flux is suppressed, and then returning to a blue-continuum sloped quasar. The model we present invokes changes at **the Innermost stable circular orbit (ISCO, defined as $r_{\rm ISCO} = \frac{6GM}{c^2}$ in the Schwarzschild metric),** to be the triggering event for substantial changes in the wider accretion disk, including major structural changes out to $150 r_g$ (where r_g is the gravitational radius; $r_g = \frac{GM}{c^2}$). Such a model explains changes in the broad emission lines, as well as the optical and IR light curves.

This paper is organised as follows. In Section 2, we describe our sample selection, catalogs and observationa data sets. In Section 3, we present various theoretical models and discuss if and how each describes and explains the data. We conclude in Section 4. We report all magnitudes on the AB zero-point system (Oke & Gunn 1983; Fukugita et al. 1996). For the WISE bands, $m_{\rm AB} = m_{\rm Vega} + m$ where $m = (2.699, 3.339)$ for WISE W1 at 3.4μm and WISE W2 at 4.6μm, respectively (Cutri et al. 2011). **We choose the cosmological parameters $\Omega_\Lambda = 0.7$, $\Omega_{\rm M} = 0.3$, and $h = 0.7$ in order to be consistent with Shen et al. (2011).**

2 TARGET SELECTION AND OBSERVATIONS

2.1 Selection in SDSS and NEOWISE-R of J1100-0053

We started by matching the SDSS Data Release 7 (DR7Q; Schneider et al. 2007) and the SDSS-III Baryon Oscillation Spectroscopic Survey (BOSS) Data Release 12 Quasar catalogues (DR12Q; Pâris et al. 2017) to the NEOWISE-R IR data. We use data from the beginning of the WISE mission (2010 January; Wright et al. 2010) through the thrid-year of NEOWISE-R operations (2016 December; Mainzer et al. 2011). The WISE scan pattern leads to coverage of the full-sky approximately once every six months (a "sky pass"), but the satellite was placed in hibernation in 2011 February and

[1] This $r^{-3/4}$ temperature dependence is not specific to the α-parametrization, and is independent from the nature of the viscosity, provided that the disk is geometrically thin, steady and heat dissipation and angular momentum transport and caused by the same, local mechanism.

[2] `legacysurvey.org/decamls/`

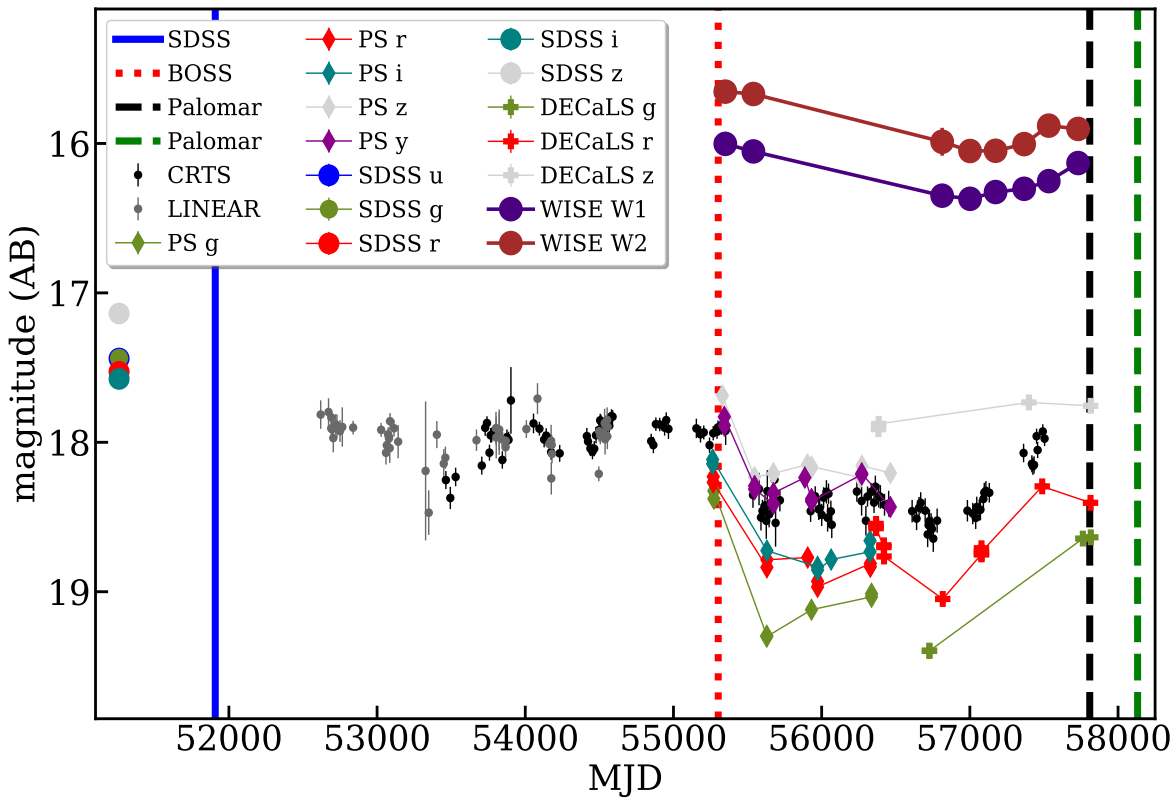

Figure 1. Multi-wavelength light curve of J1100-0053, including optical data from LINEAR, CRTS, SDSS, PanSTARRS and DECaLS, and mid-IR data from the WISE satellite. The four vertical lines illustrate the four epochs of optical spectra presented in Figure 2. J1100-0053 was flagged for further study due to the IR fading observed by WISE. Note that the optical emission has been recovering over the past few years, with the IR emission beginning to show similar behvaiour. The inserts show the images of J1100-0053 from SDSS in 1999 March and the DECaLS DR3 in 2014 March (50" on a side).

then reactivated in 2013 October. Hence, our light curves have a cadence of 6 months with a 32 month sampling gap.

The W1/W2 light curves for ~200,000 SDSS and BOSS spectroscopic quasars were obtained by performing forced photometry at the locations of DECam-detected optical sources (Lang 2014; Meisner et al. 2017b,a). This forced photometry was performed on time-resolved coadds (Lang 2014), each of which represents a stack of ~12 exposures. The coaddition removes the possibility of probing variability on $\lesssim$1 day time scales, but pushes $\approx$1.4 magnitudes deeper than individual exposures while removing virtually all single-exposure artifacts (e.g. cosmic rays and satellites).

Approximately ~30,000 of the SDSS/BOSS quasars with W1/W2 light-curves available are 'IR-bright', in that they are above both the W1 and W2 single exposure thresholds and therefore detected at very high significance in the coadds. For this ensemble of objects, the typical variation in each quasar's measured (W1-W2) color is 0.06 magnitudes. This includes statistical and systematic errors which are expected to contribute variations at the few hundredths of a magnitude level. The typical measured single-band scatter is 0.07 magnitudes in each of W1 and W2.

We undertook a search for outliers relative to these trends. Specifically, we selected objects with the following characteristics:

- Monotonic variation in both W1 and W2 flux.
- W1 flux and W2 flux Pearson correlation coefficient $r \geq 0.9$.
- >0.5 mag peak-to-peak variation in either W1 or W2.

This yields a sample of 248 sources. 31 of these are assumed to be blazars due to the presence of Faint Images of the Radio Sky at Twenty-Centimeters (FIRST; Becker et al. 1995) radio counterparts, and we discount them for further analyses. Another 22 objects are outside the FIRST footprint, leaving 195 quasars in our IR-variable sample, with no potential FIRST counterparts detected within 30".

Although aperture photometry and DECaLS forced photometry (Lang 2014; Meisner et al. 2017b,a) are available, J1100-0053 is significantly above the single-exposure detection limit so it is valid to obtain photometry from the publicly released W1/W2 Level 1b (L1b) single-exposure images at the NASA/IPAC Infrared Science Archive (IRSA). Upon querying the combined the WISE All-Sky, WISE Post-Cryo and NEOWISE-R databases, we have 101 measurements in 8 sky passes spanning nearly 2400 days.

Links to all our data, catalogs and analysis can be found online at: `github.com/d80b2t`.

2.2 Optical Imaging

Figure 1 presents the light curve of SDSS J110057.70-005304.5. J1100-0053 was first detected in the National Geographic Society-Palomar Observatory Sky Survey (NGS-POSS; Abell 1959; Minkowski & Abell 1963) in 1955 April. It is catalogued in the SuperCOSMOS Science Archive (SSA; Hambly et al. 2001a,b) and due to its equatorial position was also observed by the UK Schmidt Telescope (UKST; Cannon 1975, 1979). Querying the SSA returns *gCorMag* and *sCorMag* which are the magnitudes assuming the object is either a galaxy or star, respectively. We use the *sCorMag*

values as is appropriate for an image with flux dominated by the point-like AGN; the *sCorMag* magnitudes are calibrated in the Vega system. For J1100-0053 we find the magnitudes are: 18.10 mag in the blue UK-J filter from MJD 45440.47 (1983 April 16); 17.49 mag in the red POSS-I 'E'-filter from MJD 35214.22 (1955 April 17); 17.92 mag in the red UK-R filter from MJD 46521.47 (1986 April 01) and 17.71 mag in the UK-I filter from MJD 47273.49 (1988 April 22). J1100-0053 is not in the Digital Access to a Sky Century @ Harvard (DASCH[3]).

J1100-0053 was imaged by the Sloan Digital Sky Survey (SDSS) in the u, g, r, i and z-bands in 1999 March, and more recently by the Dark Energy Camera Legacy Survey (DECaLS) where there are 4, 13 and 4 exposures in the g, r and z-bands, respectively, in the DECaLS Data Release 3 (DR3; Dey et al. 2018). The g-band observations span ≈3 years ($56727 \leq g_{\rm MJD} \leq 57816$), while the r- and z-band observations span ≈4 years ($56367 \leq r_{\rm MJD} \leq 57814$ and $56383 \leq z_{\rm MJD} \leq 57815$).

Along with WISE IR data, optical data from the SDSS, Catalina Real-time Transient Survey (CRTS; Drake et al. 2009; Mahabal et al. 2011), the Lincoln Near-Earth Asteroid Research (LINEAR; Sesar et al. 2011) program and the Panoramic Survey Telescope and Rapid Response System (PanSTARRS; Kaiser et al. 2010; Stubbs et al. 2010; Tonry et al. 2012; Magnier et al. 2013) are also available, and presented in Fig. 1.

2.3 Additional Multiwavelength Data for J1100-0053

J1100-0053 was observed by Röntgensatellit (ROSAT) and appears in the All-Sky Survey Bright Source Catalogue (RASS-BSC; Appenzeller et al. 1998; Voges et al. 1999) as 2RXS J110058.1-005259 with 27.00 counts (count error 6.14) and a count rate = 0.06±0.01 counts s^{-1} (Boller et al. 2016). The NASA/IPAC Extragalactic Database (NED[4]) gives J1100-0053 as having a flux $1.27\pm0.28\times^{-12}$ erg cm^{-2} s^{-1} in the 0.1-2.4 keV range (unabsorbed). J1100-0053 is not in either the *Chandra* or XMM-*Newton* archives but is detected by the Galaxy Evolution Explorer (GALEX; Martin et al. 2005; Morrissey et al. 2007) and has reported flux densities 19.29 ± 0.12 mag in the far-UV and 18.89 ± 0.05 mag in the near-UV. As noted above, there is no radio counterpart within 30 arcsec in the FIRST survey, i.e. at 21cm. None of the *Hubble Space Telescope*, *Spitzer Space Telescope* or *Kepler* missions have observed J1100-0053. It is also not in the Hyper Suprime-Cam (HSC) Data Release 1 (Aihara et al. 2017) footprint.

2.4 Spectroscopy

2.4.1 SDSS and BOSS Spectroscopy

Figure 2 shows the four optical spectra of J1100-0053. J1100-0053 satisfied a number of spectroscopic targeting flags making it a quasar target in SDSS (Richards et al. 2002). An SDSS spectrum was obtained on MJD 51908 (SDSS Plate 277, Fiber 212) and the spectrum of a $z = 0.378$ quasar was catalogued in the SDSS Early Data Release (Stoughton et al. 2002; Schneider et al. 2002).

The second epoch spectrum is from the SDSS-III Baryon Oscillation Spectroscopic Survey (BOSS; Dawson et al. 2013) on MJD 55302 and shows the downturn at $\lesssim$4300Å (observed). SDSS-III BOSS actively vetoed previously known $z < 2$ quasars (Ross et al. 2012), but due to J1100-0053 being selected as an ancillary target (via a white dwarf program; Kepler et al. 2015, 2016) a second spectral epoch was obtained. Due to a design tradeoff to improve throughput in the Lyα-forest of quasar spectra in BOSS, quasar targets were subject to spectrophotometric calibration errors (Margala et al. 2016). These are introduced primarily due to offsets in fiber-hole positioning between quasar targets and spectrophotometric standard stars. However, since J1100-0053 was *not* a BOSS quasar *target*, it is not subject to this "blue offset". J1100-0053 has no pipeline flag suggesting the spectrum was compromised during data taking. We checked the calibration of BOSS Plate 3836 that observed J1100-0053 and confirmed that the data were high-SNR and that the behaviour in the blue spectrum was not due to the instrument, telescope or data reduction. **One significant aspect of the BOSS spectrum is the strong, broad Mg II emission line atop a fading red continuum. Mg II emission being prominent in objects without otherwise strong continuum is very unusual, but not unheard of. For example, Roig et al. (2014) find a group of objects with strong and broad Mg II line emission, but very weak Hα and Hβ emission, and undetectably low near-ultraviolet AGN continuum flux.**

Spectrum	SDSS	BOSS	Palomar
MJD	51908	55302	57809
Equivalent Widths			
Hγ	23	23	30
Hβ + [O III]	132	124	101
λ4959 [O III]	5	7	11
λ5007 [O III]	16	25	26
Hβ	111	92	65
[a]Hα+[NII]:	390	530	462
Line Ratios			
Hβ / (Hα + [N II])	0.36	0.27	0.18
Hγ / (Hα + [N II])	0.09	0.08	0.08
Hβ / [O III]	6.03	3.08	1.80
Hγ / Hβ	0.24	0.28	0.45

Table 1. Approximate Equivalent Width and emission line ratios for J1100-0053. Equivalent Widths are in Angstroms. [a]Estimated by extrapolating the Hα line, which is partially truncated at edge of spectrum.

2.4.2 Palomar Spectroscopy

A third epoch spectrum was obtained from the Palomar Hale 5m telescope using the Double Spectrograph (DBSP) instrument. Exposures of 600s and 300s were taken in good conditions on UT 2017 February 25 (MJD 57809). Features to note include the continuum straddling Mg II being blue in the 2017 spectrum, as it was for the SDSS spectrum in 2000, as opposed to red, as it was for the BOSS spectrum in 2010. A fourth spectral epoch was also taken using the Hale 5m and DBSP on UT 2018 January 14 (MJD 58132).

The first-epoch SDSS spectrum shows a typical blue quasar, but the blue continuum decreases by nearly a factor of ten in flux in the second epoch BOSS spectrum taken 10 years later. The blue continuum then returns in the third epoch spectrum taken another 7 years later, albeit at a diminished level relative to the initial spectrum.

We measure the emission lines using IRAF's splot task for the SDSS, BOSS and Palomar spectra and the results are presented in Table 1. We note a couple of things. First, the Hβ/[O III] line ratio has undergone a large change, decreasing by ∼3.4×.

[3] http://dasch.rc.fas.harvard.edu/project.php
[4] https://ned.ipac.caltech.edu/

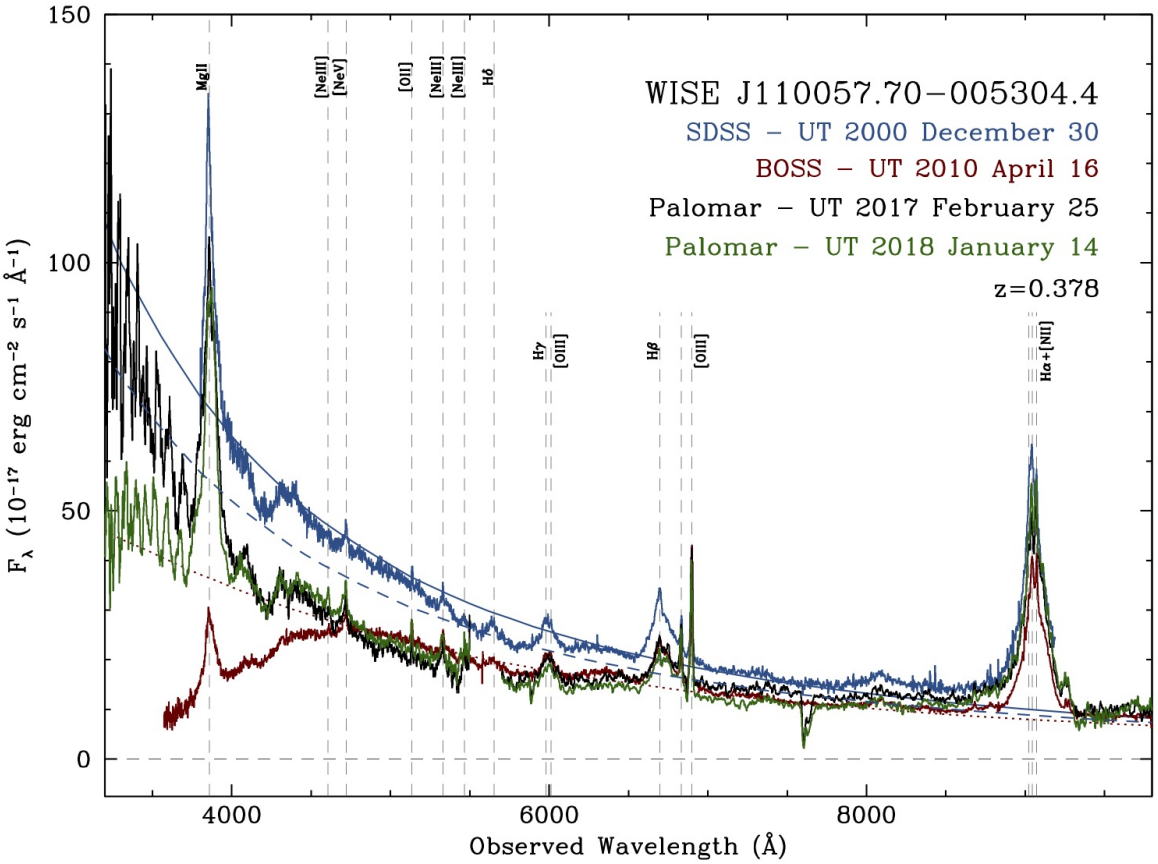

Figure 2. Optical spectra of J1100-0053 obtained on MJD 51908 (blue; SDSS), 55302 (red; BOSS), 57809 (black; Palomar) and 58132 (green; Palomar). Spectra have been renormalized to maintain a constant [O III] luminosity. Over the past two decades, the UV continuum and broad lines have changed significantly for this quasar. In particular, the 2nd-epoch BOSS spectrum from 2010 shows the rare occurrence of a temporary collapse of the UV continuum. Smooth lines show three simple thermal accretion disk models of the continuum. The solid blue line shows an inflated disk with non-zero torque at the ISCO (e.g., Sirko & Goodman 2003), while the dashed blue line shows the same model, but with zero torque at the ISCO (i.e., equivalent to a simple α-disk model, Shakura & Sunyaev 1973). Torque at the ISCO, possibly due to magnetic fields threading the inner disk and plunging region, heats the inner disk, causing it to puff up and become more UV luminous. The dotted red line shows a modified zero-torque model where the thermal disk emission interior to $80r_g$ is suppressed by a factor of 10.

Second, the Hβ equivalent width has decreased by a factor of ~1.7. This first measurements implies that the luminosity of the broad line region has significantly changed relative to the narrow line region. The second point suggests that the continuum has decreased at a different rate than the broad line emission. Despite the factor of 3.4 drop in the Hβ line flux (normalized to [O III]), the continuum only shows about 30% of this decrease. This suggests the continuum and broad lines are respond differently to mechanism driving the changes.

While continuum changes in the rest-frame UV/optical spectra of quasars are not a new discovery (see e.g., Clavel et al. 1991, the review by Ulrich et al. 1997 and more recent studies by Vanden Berk et al. 2004; Pereyra et al. 2006; MacLeod et al. 2010 and Guo & Gu 2016). However, the identification of a "UV collapse" for quasars has only recently been noted by Guo et al. (2016). Those authors report the first discovery of a UV cutoff quasar, SDSS J231742.60 +000535.1 (hereafter J2317+0005; redshift z = 0.32), observed by SDSS three times, on UT 2000 September 29, UT 2001 September 25, and UT 2001 October 18. In the case of J2317+0005, a cycle of UV emission collapse, quasar dimming, and recovery was observed over the course of just a few weeks. For J1100-0053, the cycle is far longer; however,the combination of optical and infrared light curves, as well as observing J1100-0053 at four separate spectral stages is currently unique. As such, J1100-0053 and J2317+0005 are now two archetypal objects that any accretion disk model must predict and explain (e.g., Lawrence 2018).

In our sister study, Stern et al. (2018) report on a new changing-look quasar, J1052+1519, identified with the same selection as J1100-0053, and where the broad Hβ emission has vanished compared to an archival SDSS spectrum. The physical properties of J1100-0053 derived from the MJD 51908 spectrum using the methods in Shen et al. (2011), are given in Table 2, where we also give the properties of J2317+0005 (Guo et al. 2016) and J1052+1519 (Stern et al. 2018) for comparison.

Quantity	this paper	Guo et al. (2016)	Stern et al. (2018)
SDSS name	J110057.70-005304.5	J231742.60+000535.1	J105203.55+151929.5
R.A. / deg	165.240463	349.42752075	163.01480103
Declination / deg	-0.884586	+0.093091	15.32488632
redshift, z	0.3778±0.0003	0.3209±0.0002	0.3022±0.0008
SDSS Plate, Fiber, MJD	*277, 212, 51908	*382, 173, 51816 679, 551, 52177 680, 346, 52200	*2483, 204, 53852
BOSS Plate, Fiber, MJD	3836, 258, 55302	–	–
$M_i(z=2)$ / mag	-24.48	-23.65	-22.73
log $(L_{\rm bol}/{\rm ergs}^{-1})$	45.78±0.02	45.56±0.004	45.07±0.004
log $(M_{\rm BH}/M_\odot)$	8.83±0.14	8.43±0.03	8.46±0.02
Eddington ratio (%)	7.0	10.7	3.2

Table 2. Physical properties of J1100-0053, J2317+0005 and J1052+1519 using the methods from Shen et al. (2011). *This spectrum was used to estimate the quantities reported. We use the regular definition of $L_{\rm Edd} = 4\pi G M m_{\rm p} c/\sigma_T = 1.26\times10^{38}\,(M/M_\odot)$ erg s^{-1}.

3 THEORETICAL MODELING

In a similar vein to the discussion in Stern et al. (2018), in this section we discuss several models with the aim of determining the physical mechamism(s) driving the light curve and spectral behaviour of J1100-0053. The explanations come in two broad classes: obscuration and changes in the accretion disk. Ultimately, we are forced towards a model of the latter type that combines a cooling front propagating in the accretion disk along with changes in the disk opacity.

3.1 Scenario I: Obscuration by an Infalling Cloud

We explore the possibility that an obscuring cloud, or clouds, cause the observed light curve and spectral behaviour of J1100-0053. This explanation is dismissed for the CLQ J0159+0033 in LaMassa et al. (2015) but is the preferred explanation for J2317+0005 in Guo et al. (2016).

In this scenario, the obscuring cloud(s) are required to cross the line of sight. The clouds also need to block most of the inner disk such that the ionizing radiation could not impact on the BLR or the torus for a period of months to years, in order to explain both the IR drop and broadline disappearance. An explanation of why the light curves 'recover' after a period of $\sim$ 2500 days (observed-frame) is also required; i.e., why do the light curves not rapidly return to their original flux levels once the obscuring event is over.

Clouds should not typically infall; they need to lose angular momentum if they are drawn from a distribution with Keplerian orbits, and even if they do lose angular momentum, e.g., in a collision with clouds of approximately equal mass, they would likely be either destroyed or no longer coherent. The relevant timescales here are the freefall and cloud-crushing times. The freefall timescale is

$$t_{\rm ff} \sim 100{\rm yr}\left(\frac{\rm r}{0.4{\rm pc}}\right)^{3/2}\left(\frac{\rm M}{10^8{\rm M}_\odot}\right)^{-1} \quad (1)$$

and Kelvin-Helmholtz instabilities would destroy the clouds within the cloud-crushing time, (e.g., Nagakura & Yamada 2008; Hopkins 2013; Shiokawa et al. 2015; Bae & Woo 2016), given by

$$t_{\rm cc} \sim 100{\rm yr}\left(\frac{\rho_{\rm cloud}/\rho_{\rm medium}}{10^6}\right)^{1/2}\left(\frac{\rm r_{cloud}}{4\times10^{10}{\rm km}}\right)\left(\frac{\rm v_{rel}}{10^4{\rm km/s}}\right)^{-1}. \quad (2)$$

Thus, even if clouds did infall, they would end up fragmented, which should pollute the inner disk. The dust in the cloud would then be well inside the dust sublimation radius

$$R_{\rm dust} \approx 0.4{\rm pc}\left(\frac{\rm L}{10^{45}{\rm erg/s}}\right)^{1/2}\left(\frac{\rm T_{sub}}{1500{\rm K}}\right)^{2.6} \quad (3)$$

and so the dust will be destroyed in the $\sim$100 year free-fall from the dust-sublimation region. Hence, one can not absorb the UV spectrum with dust, since it will have been sublimated well before it arrives at the inner disk.

3.2 Scenario II: Accretion Disk Model

Having discounted an obscuring event as the explanation for J1100-0053, we turn to accretion disk models (see also the recent review by Yuan & Narayan 2014). We consider 'cold' accretion flows, described as optically thick, geometrically thin and which drive relatively high mass accretion rates. They are 'cold' in the sense that the virial temperature of particles near the black hole is low. Similarly, we characterize optically thin, geometrically thick and low mass accretion rate flows as virially 'hot' accretion flows.

After giving our model set-up, we discuss whether J1100-0053 can be described by a 'hot' accretion flow, such as the advection-dominated accretion flow. We then discuss our preferred 'cold' accretion flow model, but where the temperature of the accretion disk is perturbed by propagating cooling and heating fronts in the inner parts ($\leq 1000 r_g$) of the accretion disk. Our disk remains virially cold throughout this cycle.

We start with a multi-temperature blackbody (MTB) model, with a $L \propto T^4$ dependence and a $T \propto r^{-3/4}$ relation. A thin accretion disk has a negligible radial pressure gradient. Therefore, at each radius R the gas orbits at the Keplerian angular frequency, $\Omega_{\rm K} = (GM/r^3)^{1/2}$, where M is the mass of the central object and possesses specific angular momentum $l = \sqrt{GMr}$.

Zimmerman et al. (2005) compare models with 'zero' and 'non-zero' torque at the ISCO, and the impact on the temperature profile of the corresponding accretion disk, when the torque changes. From Zimmerman et al. (2005) the zero torque (ZT)

luminosity is given by

$$L_{\rm disk} = \frac{GM\dot{M}}{2r_{\rm in}} = 73.9\sigma \left(\frac{T_{\rm max}}{f}\right)^4 r_{\rm in}^2 \quad (4)$$

and the standard, non-zero torque (NZT) luminosity is given by:

$$L_{\rm disk} = \frac{3GM\dot{M}}{2r_{\rm in}} = 12.6\sigma \left(\frac{T_{\rm max}}{f}\right)^4 r_{\rm in}^2 \quad (5)$$

In zero-torque models, temperature $T_{\rm ZT}$ goes to zero at the inner edge of the disk (since the torque vanishes there) whereas a non-zero torque temperature profile, $T_{\rm NZT}$ reaches its maximum value at the inner edge of the disk (where the torque is maximal). Given a MTB model for disk emission, these differences at small $r_{\rm g}$ translate to large differences in the SED.

As in shown in Figure 3, the SDSS spectrum from 2000 is well fit with a thin Shakura & Sunyaev (1973) α-disk and the NZT condition. However, just switching to just the ZT condition, while surpressing the bluer disk emissivity, is not sufficient to explain the 2010 spectrum.

3.2.1 Switching States to a RIAF/ADAFs:

A possible explanation for the behaviour of J1100-0053 is that it switches accretion modes, from a virially cold, high $\dot{M}$ flow to a virially hot, lower $\dot{M}$ flow, with the latter being, i.e., a radiatively inefficient accretion flow (RIAF; Narayan et al. 1998; Quataert 2001) or an advection-dominated accretion flow (ADAF; Yuan & Narayan 2014, and references therein).

There are examples of this type of behaviour in lower-luminosity objects. For example, Nemmen et al. (2006) successfully explain the SED for the low-ionization nuclear emission-line region (LINER) of NGC 1097 with a model where the inner part of the flow is a virially hot RIAF, and the outer part as a standard virially cold thin disk.

The broadband spectrum of NGC 1097 from Nemmen et al. (2006) initially appears similar to the UV/optical 2010 spectrum of J1100-0053. Figure 4 in Nemmen et al. (2006) shows the MTB-like model component from the thin disk at $r > 225r_g$ (their long dashed line) dramatically decreasing at $\sim 10^{15}$Hz (~300nm). Nemmen et al. (2006) model the disk region interior to this as a RIAF[5] at a power (in νL_ν), an order of magnitude lower than the MTB in the optical, but spanning from the X-ray to the far-IR.

Can J1100-0053 switch states from a thin disk quasar to an ADAF at small radii with the thin disk surviving at large radii? Assuming the transition happens due to a thermal instability in the inner disk on the thermal timescale, and propagates outwards to radii $\sim 225r_g$ as in Nemmen et al. (2006), we can parameterize the front propagation time as

$$t_{\rm front} \sim 5 \text{ yrs} \left(\frac{h/r}{0.1}\right)^{-1} \left(\frac{\alpha}{0.3}\right)^{-1} \left(\frac{r}{225r_g}\right)^{3/2} \frac{r_g}{c} \quad (6)$$

where we have had to assume a higher value of $\alpha \sim 0.3$ (King et al. 2007) than typically assumed for thin ($h/r \ll 1$) disks. This is plausible if there exists a very viscous disk and the effect propagates outwards on a timescale of ≤ 5 years from the inner disk.

[5] A change to an advection-dominated accretion flow (ADAF) is also possible in this model.

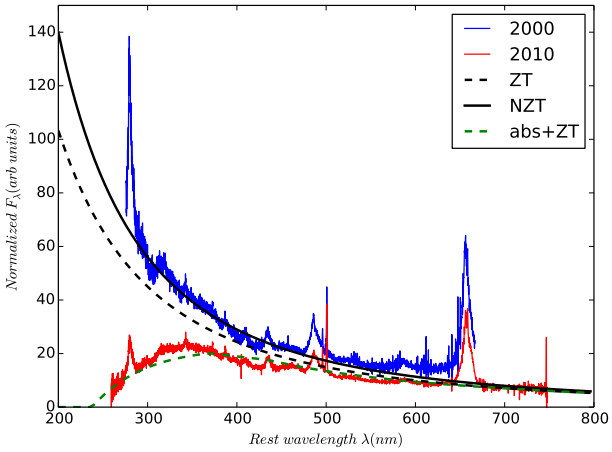

Figure 3. J1100-0053 data (blue line 2000 spectrum; red line 2010 spectrum) and 4 models. The solid black line shows non-zero torque at ISCO (following Afshordi & Paczyński 2003) while the dashed black line shows a zero torque at the ISCO with a no absorption model. The green dashed line as a zero torque at the ISCO model multiplied by an absorption law adapted from (Guo et al. 2016).

If the viscous disk switches to a RIAF at radii $<225r_g$, then the UV/optical emission should be supressed by several orders of magnitude compared to a radiatively efficient thin disk (Narayan et al. 1998; Abramowicz et al. 2002; Abramowicz & Fragile 2013). However, if the thin disk emission is simply uniformly suppressed within $< 225r_g$ by a large factor, we cannot reproduce the shape of the 2010 J1100-0053 spectrum. Furthermore, in order to restore the thin disk in the 2016 observation, a thermal instability is required to occur at $\sim 225r_g$ and a front to propagate inwards, collapsing the RIAF back to a thin disk.

Noting RIAFs/ADAFs exist at lower luminosity than for a classic thin disk ($\epsilon \sim 0.005$ and $\epsilon \sim 0.1$, respectively, for $L = \epsilon \dot{M} c^2$) it is unclear first what physical processes would trigger the change of state to an ADAF and then cool back down to a thin disk, and second, why such an instability would occur at the thin disk/RIAF boundary in J1100-0053, whereas in NGC 1097 this interface appears to be stable. In any case, suppressing the MCD temperature profile inside a radius of $r_{\rm alt} = 225r_g$ leads to a collapse in the total flux compared to unperturbed disk. These scenarios are difficult to reconcile with our data.

3.2.2 Propagation of a Cooling Front:

Alternatively, a phenomenological explanation of the sequence of our observations consists of a triggering event at the ISCO which cools the inner disk and leads to the radial propagation outward of a cooling front. At large radii, a heating front returns, re-inflating the disk. This simple model, and our preferred model here, is outlined in cartoon form in Figure 4.

Our explanation for the behaviour of J1100-0053 (and J2317+0005), starts from the more-realistic, but α-parameterized disk model of Sirko & Goodman (2003). In their model, the outer accretion disk is heated sufficiently to maintain stability against gravitational collapse, and small changes in temperature can lead to large changes in opacity and thus disk luminosity. In addition, the theoretical SEDs have a second peak in the near-infrared that is energetically comparable with

the Big Blue Bump. Sirko & Goodman (2003) assume that the viscous torque at the inner edge of their accretion disks is vanishingly small and effectively zero. This is a good assumption *as long as there is no connection between material inside the ISCO, i.e. the plunging region, and material at the ISCO*.

An initially modestly fat disk ($h/r \sim 0.2$) with a modest α, cools from the ISCO and propagates outward in a cooling front, collapsing the disk. The cooling (or indeed heating) front propagates radially through an α-parameterized disk at approximately the sound speed c_s multiplied by α (e.g., Eqn. 20 from Hameury et al. 2009)

$$v_{\rm front} = \alpha c_{\rm s} \tag{7}$$

As the hot disk ($\sim 10^{5-6}$K) cools, it fragments into cooler clumps around $\sim 10^4$K (see e.g., McCourt et al. 2016). Let us assume the cold phase clumps occur on size-scales of order r_g, with an overdensity of 10^4 relative to their surroundings, and a relative velocity compared to the hot phase around them on the order of the orbital velocity. Then, the cold phase clumps are unstable to the Kelvin-Helmholtz instability (Eqn. 2) relative to their surroundings on an approximate timescale of

$$t_{\rm cc} \approx 3{\rm mo} \left(\frac{\rho_{\rm cloud}/\rho_{\rm medium}}{10^4}\right)^{1/2} \left(\frac{r_{\rm cloud}}{r_g}\right) \left(\frac{v_{\rm rel}}{10^4 {\rm kms}^{-1}}\right)^{-1}. \tag{8}$$

Our parameterization may not be particularly accurate but it is illustrative. *The important point is that any cold phase clouds must vanish after a relatively short time unless they are extremely over-dense with very cold cores relative to the surrounding medium.*

The main coolants $> 10^{4.5}$K are resonance lines in Carbon and Oxygen and at lower temperatures, H and He from neutral phase material (see e.g., Fig. 18 in Sutherland & Dopita 1993). The ionization energies for carbon and oxygen are 11.26 and 13.61 eV, respectively, i.e., $\sim$ 100nm, and hence at wavelengths $<$ 100nm the disk opacity will increase dramatically in an edge. However, the gas in the disk is pressure, turbulence and Doppler broadened, so these ionization edges will manifest around 100nm with decreasing opacity to shorter wavelengths as

$$\kappa \propto \rho T^{-1/2} \nu^{-3} \tag{9}$$

for Kramers' opacities. This implies $\kappa \propto \lambda^3$ at increasing wavelengths up to the ionization edge around 100nm. These features will be blurred (by the broadening) and the ionization edges due to the C and O resonance lines in the cool phase of this disk will be span 50 – 200nm, depressing the flux at these energies. We note this closely resembles the opacity curve inferred by Guo et al. (2016) in J2317+0005 over relevant wavelengths.

The 2010 spectrum in this model comes from a cooler disk plus the increased opacity at short wavelengths in the cooler phase. Heating occurs from the outside in, explaining the 2016 spectrum and asymmetric recovery in photometry. Since the optical continuum has been rising again since mid-2016, this leads to a prediction of a rise in Hydrogen emission line flux in the next few months. The infrared flux returns in 2021.

However, if accretion disk luminosity is powered by magnetized gas losing angular momentum, it is reasonable to assume that magnetic fields are dragged across the ISCO with accreting matter, into the plunging region. As a result, we should typically expect a non-zero torque at the ISCO, as the magnetized plunging gas torques the ISCO gas. A drop in the torque at the ISCO is then most likely due to a change in $\dot{M}$ at the ISCO, which could result from a local change in α or a stochastic variation in the mass supply. We can regard this as the "the triggering event".

A non-zero torque at the ISCO implies that matter in the plunging region is connected (however weakly) to matter outside the ISCO, probably by magnetic fields Gammie (e.g., 1999); Agol & Krolik (e.g., 2000). A non-zero torque at the ISCO maintains a hotter innermost disk than a condition of zero torque at the ISCO, and an assumption of non-zero torque is particularly appropriate if disk viscosity and accretion are driven by magnetic fields. Our model of thermal emission from a MTB implies changes in the region from the ISCO to ~few tens-100 $r_{\rm g}$ are required to suppress flux into the observed g-band.

In particular, we suggest a physical collapse of the disk scale height due to a cooling front propagating outward from the ISCO. The radiation properties of accretion disk with a NZTs at their inner edge was also explored by Cao & Xu (2003) and Cannizzo (1998b) describe in detail, the change at the ISCO is physically related to this thermal front.

We note that Hameury et al. (2009) investigate thermal-viscous instabilities in AGN, and find that a physical mechanism of propogating cooling and heating fronts is found, and that these fronts propagate on much shorter time scales than the viscous time. The model in Hameury et al. (2009) makes a firm prediction of this back and forth propagation of cooling and heating fronts on a short time scale, while noting that the surface density at smaller radii does not change so quickly and hence $\dot{M}$ fluctuates on a longer timescale.

As noted above, one simple, plausible trigger for this cooling front is that the non-zero torque condition at theISCO changes to a (more nearly) zero-torque condition. This dramatic decrease in the torque at the ISCO leads to a drastically cooler, thinner innermost disk. As the cooling front propagates, the drop in temperature leads to a drop in flux. To fit the observed spectra, our model has the cooler regions behind the front emitting 10% the flux of the initial hotter disk, and assumes the disk height drops by a factor ~2. The dimming of the inner disk causes a drop in the ionizing photon flux, which will cause the Balmer lines to drop in flux after a light travel time of months and the IR emission from the outer disk/torus to drop in flux after a light travel time of ~3 years (Sirko & Goodman 2003; Koshida 2014; Jun et al. 2015).

If the inner accretion disk is usually inflated Sirko & Goodman (see e.g., 2003); Thompson et al. (see e.g., 2005); Hopkins & Quataert (see e.g., 2011), such a cooling front will naturally produce a collapse in the disk scale height, triggering a decrease in flux moving from UV to longer optical wavelengths, and a temporarily thicker scattering atmosphere, further decreasing flux at short wavelengths (see Fig. 4). Given our disk parameters, outward front propagation timescales are months-to-years, corresponding with observed timescales for optical emission moving from shorter to longer wavelengths as the radius of the cooling front increases. A decrease in the UV flux would be expected to cause a decrease in IR flux, as the heating of the IR-emitting dusty torus is reduced; however, there should be a delay due to light travel time Jun et al. (e.g., 2015). By 2010 (MJD 55300) the front has reached $r \sim 50 r_g$. During that time, the collapsing disk height increases the number density of scatterers and the temporary cold phase formed at the disk surface produces the remarkable blue downturn in the 2010 spectrum. The cooling front continues to propagate radially outward but cools less efficiently at larger disk radii.

Eventually, very much in the same vein as discussed by Hameury et al. (2009), somewhere in the disk, Σ reaches the critical surface density $\Sigma_{\rm max}$, and that triggers the heating instability. A heating front propagates back inwards, analagous to the well-known accretion disk limit cycle mechanism in models of dwarf novae outbursts (e.g., Cannizzo 1998a). The returning heating front

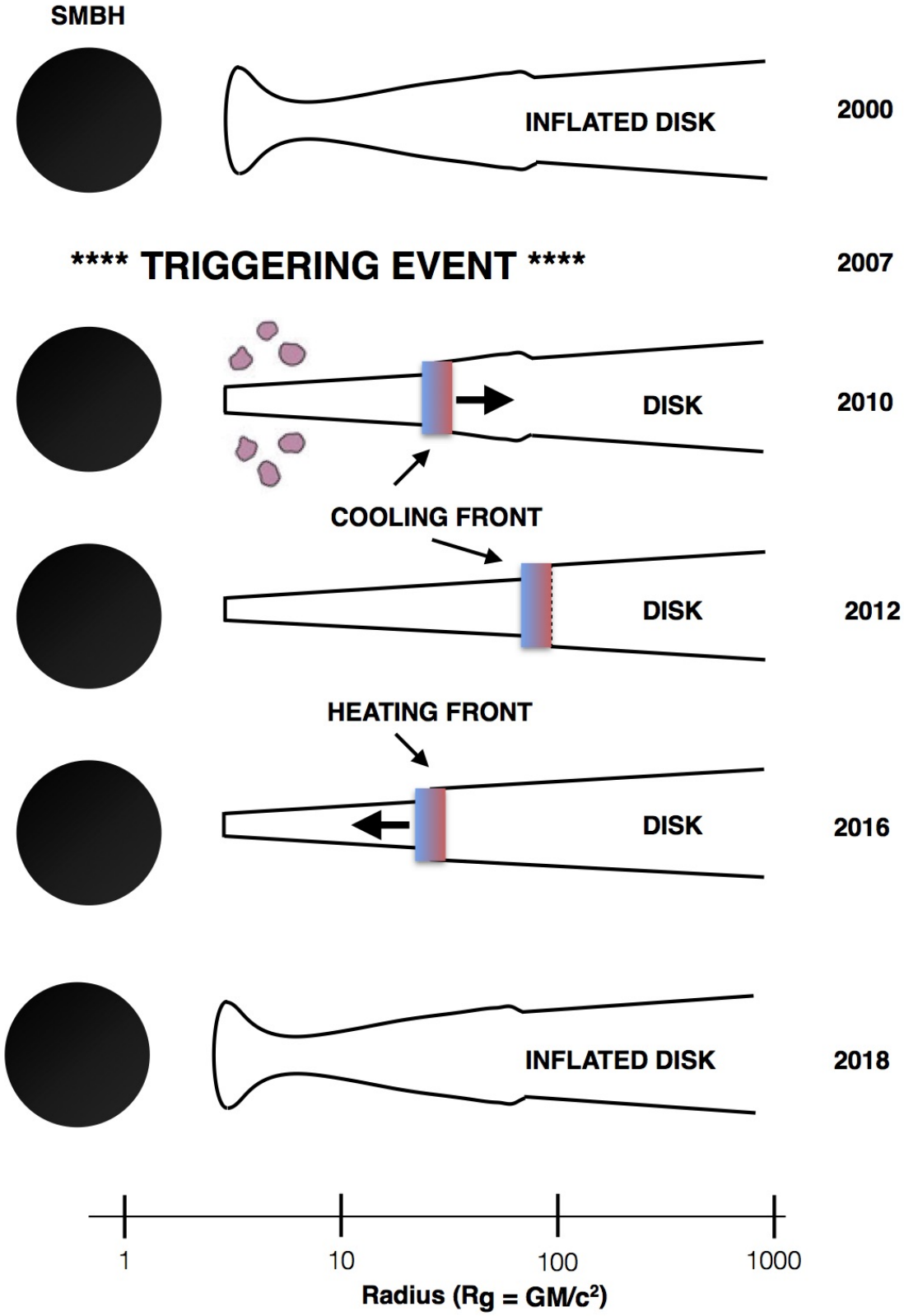

Figure 4. Cartoon illustration of our model explaining the unusual spectral evolution of J1100-0053. In 2000, corresponding to the SDSS spectral epoch, the quasar has a standard inflated accretion disk, i.e., where non-zero torque at the ISCO heats the inner radii of the accretion disk, causing it to puff up (e.g., Zimmerman et al. 2005). Circa 2007, a triggering event occurs that deflates the inner disk, possibly due to a shift in the magnetic field configuration leading to zero torque at the ISCO. This event leaves some scattering clouds, and causing a cooling front to propagate outwards in the accretion disk, traveling on the $t_{\rm front}$ time-scale (see also Hameury et al. 2009). Circa 2012, the cooling front reaches a predicted kink in the accretion disk profile at ~100 r_g, associated with a shift in the accretion disk opacity, e.g., Figure 2 of Sirko & Goodman (2003). A heating front then travels radially inwards, re-heating the inner accretion disk but on longer timescales, due to the thinner disk. We predict that in the next year, the quasar should roughly return to its initial state.

travels more slowly because the disk is thinner (and $t_{\rm front}$ is inversely proportional to h/r) and will re-inflate the disk as it propagates inwards towards the SMBH. This means the return to normal will be asymmetric in time, as observed, and the shortest wavelength bands bottom out first, because that wavelength is dominated by emission coming from $r \sim 100 r_g$.

Using Ford et al. (2018) and Sirko & Goodman (2003), Figure 4 shows a model for a $M_{\rm BH} = 7 \times 10^8 M_\odot$, with an accretion rate in units of Eddington accretion, $\dot{M} = 0.070$ (appropriate for J1100-0053), radiative efficiency of $\epsilon = 0.1$ inner disk radius of $6r_{\rm g}$ and outer disk radius of $10{,}000 r_g$. The resulting model spectra can be seen in Figure 2. We expect the front to return to the ISCO in mid-to-late 2018. That means the broad Balmer lines will come back a few months later, but the WISE IR flux should return to full flux in 2021. We note the IR brightness of J2317+0005 was only observed at one epoch and the change in the UV for J2317+0005 was rapid, decreasing by a factor of 3.5 at 3000Å over only 23 days. This indicates that the cooling event was very brief, and given the extremal but plausible values of $h/r = 0.2 - 0.3$ and $r = 20 - 25$ with α held at 0.3, is consistent with our model.

4 CONCLUSIONS

By monitoring changing look quasars we introduce new tests of models of accretion disk physics. We present the quasar J1100-0053 that was catalogued in the Sloan Digital Sky Survey quasar survey, but identified as an interesting due to its near-infrared photometric properties.

We have shown that a simple phenomenological model with a propagating cooling front is capable of describing the gross spectral and temporal variations in a changing looking quasar. Our model makes a prediction for this source, testable over the next few years and, if confirmed, implies that changing looking quasars as a class are driven by changes near the ISCO, close to the SMBH. The discovery of J1100-0053 (and J2317+0005) are specific key examples of time-domain astronomy and the resulting astrophysics to be studied. However, even with the coverage from WISE, PanSTARRS, SDSS, DECaLS and CRTS, we have a relatively sparse dataset which cannot tightly constrain our theoretical model.

The Zwicky Transient Facility (ZTF; Bellm 2014) has very recently started and will open a new data space with high cadence, multi-band photometric monitoring. Along with ZTF in the very near future, the Large Synoptic Survey Telescope (Ivezic & Tyson 2008; LSST Science Collaborations et al. 2009) will allow identification of the types of events such as J1100-0053 and J2317+0005 *while they are occurring*, allowing spectroscopic monitoring. We will be able to see how long a UV collapse lasts and closely follow its evolution. Such data will stringently test models of AGN disks at much higher fidelity than we are able to do with current 'Changing-Look' quasar samples.

Author Contributions. N.P.R. led the project, developed and wrote the initial drafts of the manuscript and co-ordinated the team. K.E.S.F. and B.K. orginated and developed the theoretical interpretation presented here. M.G. and D.S. were heavily responsible for the initial discussions and observations that were the genesis of this project. A.M.M. produced the initial infrared variable quasar catalogs. D.S., M.G. and A.J.D. were part of the Palomar observing team. N.P.R., A.M.M. and A.D. are part of the DECaLS Legacy Survey. R.A., A.D. and H.D.J. contributed to the manuscript.

Availability of Data and computer analysis codes. All materials, data, code and analysis algorithms are fully available at: https://github.com/d80b2t/WISE_LCs

ACKNOWLEDGEMENTS

NPR acknowledges support from the STFC and the Ernest Rutherford Fellowship scheme. KESF & BM are supported by NSF PAARE AST-1153335. KESF & BM thank CalTech/JPL for support during sabbatical. MF acknowledges support from NSF grants AST-1518308, AST-1749235, AST-1413600 and NASA grant 16-ADAP16-0232. RJA was supported by FONDECYT grant number 1151408. AMM acknowledges support from NASA ADAP grant NNH17AE75I.

We thank David J. Schlegel for quality checks on the BOSS data, and Chris Done for invigorating discussions at the concept and conclusion of this work.

This publication makes use of data products from the Wide-field Infrared Survey Explorer, which is a joint project of the University of California, Los Angeles, and the Jet Propulsion Laboratory/California Institute of Technology, and NEOWISE, which is a project of the Jet Propulsion Laboratory/California Institute of Technology. WISE and NEOWISE are funded by the National Aeronautics and Space Administration.

This research has made use of the NASA/IPAC Extragalactic Database (NED) which is operated by the Jet Propulsion Laboratory, California Institute of Technology, under contract with the National Aeronautics and Space Administration.

This research has made use of data obtained from the SuperCOSMOS Science Archive, prepared and hosted by the Wide Field Astronomy Unit, Institute for Astronomy, University of Edinburgh, which is funded by the UK Science and Technology Facilities Council.

The GALEX GR6/7 Data Release hosted at http://galex.stsci.edu/GR6/ was used. These data were obtained from the Mikulski Archive for Space Telescopes (MAST). STScI is operated by the Association of Universities for Research in Astronomy, Inc., under NASA contract NAS5-26555. Support for MAST for non-HST data is provided by the NASA Office of Space Science via grant NNX09AF08G and by other grants and contracts.

Funding for SDSS-III has been provided by the Alfred P. Sloan Foundation, the Participating Institutions, the National Science Foundation, and the U.S. Department of Energy Office of Science. The SDSS-III web site is http://www.sdss3.org/. SDSS-III is managed by the Astrophysical Research Consortium for the Participating Institutions of the SDSS-III Collaboration including the University of Arizona, the Brazilian Participation Group, Brookhaven National Laboratory, Carnegie Mellon University, University of Florida, the French Participation Group, the German Participation Group, Harvard University, the Instituto de Astrofisica de Canarias, the Michigan State/Notre Dame/JINA Participation Group, Johns Hopkins University, Lawrence Berkeley National Laboratory, Max Planck Institute for Astrophysics, Max Planck Institute for Extraterrestrial Physics, New Mexico State University, New York University, Ohio State University, Pennsylvania State University, University of Portsmouth, Princeton University, the Spanish Participation Group, University of Tokyo, University of Utah, Vanderbilt University, University of Virginia, University of Washington, and Yale University.

REFERENCES

Abell G. O., 1959, Leaflet of the Astronomical Society of the Pacific, 8, 121
Abramowicz M. A., Fragile P. C., 2013, Living Reviews in Relativity, 16, 1
Abramowicz M. A., Igumenshchev I. V., Quataert E., Narayan R., 2002, ApJ, 565, 1101
Afshordi N., Paczyński B., 2003, ApJ, 592, 354
Agol E., Krolik J. H., 2000, ApJ, 528, 161
Aihara H., et al., 2017, preprint, (arXiv:1702.08449)
Alloin D., Pelat D., Phillips M., Whittle M., 1985, ApJ, 288, 205
Antonucci R., 1993, ARA&A, 31, 473
Appenzeller I., et al., 1998, ApJS, 117, 319
Assef R. J., Stern D., Noirot G., Jun H. D., Cutri R. M., Eisenhardt P. R. M., 2018, ApJS, 234, 23
Bae H.-J., Woo J.-H., 2016, ApJ, 828, 97
Balbus S. A., Hawley J. F., 1991, ApJ, 376, 214
Becker R. H., White R. L., Helfand D. J., 1995, ApJ, 450, 559
Begelman M. C., McKee C. F., Shields G. A., 1983, ApJ, 271, 70
Bellm E., 2014, in Wozniak P. R., Graham M. J., Mahabal A. A., Seaman R., eds, The Third Hot-wiring the Transient Universe Workshop. pp 27–33 (arXiv:1410.8185)
Boller T., Freyberg M. J., Trümper J., Haberl F., Voges W., Nandra K., 2016, A&A, 588, A103
Cannizzo J. K., 1998a, ApJ, 493, 426
Cannizzo J. K., 1998b, ApJ, 494, 366
Cannon R. D., 1975, Proceedings of the Astronomical Society of Australia, 2, 323
Cannon R. D., 1979, The U.K. 1.2m Schmidt telescope and the southern sky survey
Cao X., Xu Y.-D., 2003, PASJ, 55, 149
Clavel J., et al., 1991, ApJ, 366, 64
Cutri R. M., et al., 2011, Technical report, Explanatory Supplement to the WISE Preliminary Data Release Products
Dawson K., et al., 2013, AJ, 145, 10
Dey A., et al., 2018, preprint, (arXiv:1804.08657)
Drake A. J., et al., 2009, ApJ, 696, 870
Elvis M., et al., 1994, ApJS, 95, 1
Ford K. E. S., et al., 2018, in prep.
Fukugita M., Ichikawa T., Gunn J. E., Doi M., Shimasaku K., Schneider D. P., 1996, AJ, 111, 1748
Gammie C. F., 1999, ApJ, 522, L57
Guo H., Gu M., 2016, ApJ, 822, 26
Guo H., et al., 2016, ApJ, 826, 186
Hambly N. C., et al., 2001a, MNRAS, 326, 1279
Hambly N. C., Irwin M. J., MacGillivray H. T., 2001b, MNRAS, 326, 1295
Hameury J.-M., Viallet M., Lasota J.-P., 2009, A&A, 496, 413
Hopkins P. F., 2013, MNRAS, 428, 2840
Hopkins P. F., Quataert E., 2011, MNRAS, 415, 1027
Ivezic Z., Tyson J. A. f., 2008, preprint, (arXiv:0805.2366)
Jun H. D., Stern D., Graham M. J., Djorgovski S. G., Mainzer A., Cutri R. M., Drake A. J., Mahabal A. A., 2015, ApJ, 814, L12
Kaiser N., et al., 2010, in Society of Photo-Optical Instrumentation Engineers (SPIE). p. 0, doi:10.1117/12.859188
Kepler S. O., et al., 2015, MNRAS, 446, 4078
Kepler S. O., et al., 2016, MNRAS, 455, 3413
King A., 2012, Mem. Soc. Astron. Italiana, 83, 466
King A. R., Pringle J. E., Livio M., 2007, MNRAS, 376, 1740
Koratkar A., Blaes O., 1999, PASP, 111, 1
Koshida S. o., 2014, ApJ, 788, 159
LSST Science Collaborations et al., 2009, preprint, (arXiv:0912.0201)
LaMassa S. M., et al., 2015, ApJ, 800, 144
Lang D., 2014, AJ, 147, 108
Lasota J.-P., 2016, in Bambi C., ed., Astrophysics and Space Science Library Vol. 440, Astrophysics of Black Holes: From Fundamental Aspects to Latest Developments. p. 1 (arXiv:1505.02172v3), doi:10.1007/978-3-662-52859-4_1
Lawrence A., 2012, MNRAS, 423, 451
Lawrence A., 2018, Nature Astronomy, 2, 102
Lusso E., Risaliti G., 2017, A&A, 602, A79
MacLeod C. L., et al., 2010, ApJ, 721, 1014
MacLeod C. L., Ross N. P., et al., 2016, MNRAS, 457, 389
Magnier E. A., et al., 2013, ApJS, 205, 20
Mahabal A. A., et al., 2011, Bulletin of the Astronomical Society of India, 39, 387
Mainzer A., et al., 2011, ApJ, 731, 53
Mainzer A., et al., 2014, ApJ, 792, 30
Malkan M. A., Sargent W. L. W., 1982, ApJ, 254, 22
Margala D., Kirkby D., Dawson K., Bailey S., Blanton M., Schneider D. P., 2016, ApJ, 831, 157
Martin D. C., et al., 2005, ApJ, 619, L1
McCourt M., Oh S. P., O'Leary R. M., Madigan A.-M., 2016, preprint, (arXiv:1610.01164)
McKernan B., Ford K. E. S., Kocsis B., Lyra W., Winter L. M., 2014, MNRAS, 441, 900
Meisner A. M., Bromley B. C., Nugent P. E., Schlegel D. J., Kenyon S. J., Schlafly E. F., Dawson K. S., 2017a, AJ, 153, 65
Meisner A. M., Lang D., Schlegel D. J., 2017b, AJ, 154, 161
Minkowski R. L., Abell G. O., 1963, The National Geographic Society-Palomar Observatory Sky Survey. the University of Chicago Press, p. 481
Morgan C. W., Kochanek C. S., Morgan N. D., Falco E. E., 2010, ApJ, 712, 1129
Morgan C. W., et al., 2012, ApJ, 756, 52
Morrissey P., et al., 2007, ApJS, 173, 682
Mosquera A. M., Kochanek C. S., 2011, ApJ, 738, 96
Nagakura H., Yamada S., 2008, ApJ, 689, 391
Narayan R., Mahadevan R., Quataert E., 1998, in Abramowicz M. A., Björnsson G., Pringle J. E., eds, Theory of Black Hole Accretion Disks. pp 148–182 (arXiv:astro-ph/9803141)
Nemmen R. S., Storchi-Bergmann T., Yuan F., Eracleous M., Terashima Y., Wilson A. S., 2006, ApJ, 643, 652
Oke J. B., Gunn J. E., 1983, ApJ, 266, 713
Pâris I., Petitjean P., Ross N. P., et al., 2017, A&A, 597, A79
Pereyra N. A., Vanden Berk D. E., Turnshek D. A., Hillier D. J., Wilhite B. C., Kron R. G., Schneider D. P., Brinkmann J., 2006, ApJ, 642, 87
Perlman E., Addison B., Georganopoulos M., Wingert B., Graff P., 2008, in Blazar Variability across the Electromagnetic Spectrum. p. 9 (arXiv:0807.2119v2)
Pooley D., Blackburne J. A., Rappaport S., Schechter P. L., 2007, ApJ, 661, 19
Pringle J. E., 1981, ARA&A, 19, 137
Quataert E., 2001, in Peterson B. M., Pogge R. W., Polidan R. S., eds, Astronomical Society of the Pacific Conference Series Vol. 224, Probing the Physics of Active Galactic Nuclei. p. 71
Richards G. T., et al., 2002, AJ, 123, 2945
Richards G. T., et al., 2006, ApJS, 166, 470
Risaliti G., Young M., Elvis M., 2009, ApJ, 700, L6
Roig B., Blanton M. R., Ross N. P., 2014, ApJ, 781, 72
Ross N. P., et al., 2012, ApJS, 199, 3
Ruan J. J., et al., 2016, ApJ, 826, 188
Rumbaugh N., et al., 2017, preprint, (arXiv:1706.07875v1)
Runnoe J. C., et al., 2016, MNRAS, 455, 1691
Schneider D. P., et al., 2002, AJ, 123, 567
Schneider D. P., et al., 2007, AJ, 134, 102
Sesar B., Stuart J. S., Ivezić Ž., Morgan D. P., Becker A. C., Woźniak P., 2011, AJ, 142, 190
Shakura N. I., Sunyaev R. A., 1973, A&A, 24, 337
Shen Y., et al., 2011, ApJS, 194, 45
Shields G. A., 1978, Nature, 272, 706
Shiokawa H., Krolik J. H., Cheng R. M., Piran T., Noble S. C., 2015, ApJ, 804, 85
Sirko E., Goodman J., 2003, MNRAS, 341, 501
Stern D., et al., 2018, ApJ, submitted
Stoughton C., et al., 2002, AJ, 123, 485
Stubbs C. W., et al., 2010, ApJS, 191, 376
Sutherland R. S., Dopita M. A., 1993, ApJS, 88, 253

Thompson T. A., Quataert E., Murray N., 2005, ApJ, 630, 167
Tonry J. L., et al., 2012, ApJ, 750, 99
Ulrich M.-H., Maraschi L., Urry C. M., 1997, ARA&A, 35, 445
Vanden Berk D. E., et al., 2004, ApJ, 601, 692
Voges W., et al., 1999, A&A, 349, 389
Wright E. L., et al., 2010, AJ, 140, 1868
Yang Q., et al., 2017, preprint, (arXiv:1711.08122v1)
Yuan F., Narayan R., 2014, ARA&A, 52, 529
Zimmerman E. R., Narayan R., McClintock J. E., Miller J. M., 2005, ApJ, 618, 832

This paper has been typeset from a TEX/LATEX file prepared by the author.